JOURNAL OF GEOPHYSICAL RESEARCH, VOL. 90, NO. C4, PAGES 6945–6952, JULY 20, 1985

A Meridional ^{14}C and ^{39}Ar Section in Northeast Atlantic Deep Water

REINER SCHLITZER AND WOLFGANG ROETHER

Intitut für Umweltphysik, Universität Heidelberg, Federal Republic of Germany

URS WEIDMANN, PETER KALT, AND HEINZ HUGO LOOSLI

Physikalisches Institut, Universität Bern, Switzerland

^{14}C, ^{39}Ar, and complementary hydrographic and nutrient data are presented for deep water below 2500 m depth, from stations along a meridional section (8°S to 45°N) through the Romanche Trench and along the deep northeast Atlantic basins (F/S *Meteor*, cruise 56, leg 5). The large-scale ^{14}C distribution along the section is resolved at the ^{14}C data precision of ±2‰. Bottom water $\Delta^{14}C$ decreases by 6‰ from the equator to 45°N, and farther up there is a weak $\Delta^{14}C$ minimum (−123‰) over much of the section. The ^{14}C data are interpreted as giving a turnover time of about 30 years for the waters below the depth of the ^{14}C minimum (~4250 m). It is found that water of 1.50 ± 0.05°C potential temperature enters the East Atlantic from the west through the Romanche Trench (sill depth about 4000 m), and a preliminary value for the inflow rate of 3.6×10^6 m^3/s is deduced. This rate greatly exceeds estimated deep inflow rates through the Vema fracture zone or across the northern boundary of the East Atlantic. ^{39}Ar data that cover an entire deep-ocean circulation system are presented for the first time. The observed ^{14}C and ^{39}Ar distributions are mutually consistent. Transit times from the source regions to the equator for water from northern and southern deepwater sources are estimated to be about 170 and 105 years, respectively, and the ^{39}Ar concentration of young Antarctic Bottom Water is deduced as 60 ± 7% modern. The ^{39}Ar-^{14}C correlation in the ocean appears to be affected by mixing of waters of different age and by more efficient raising of ^{39}Ar in the deepwater formation processes.

1. INTRODUCTION

In April 1981 the F/S *Meteor* completed a long meridional section (8°S to 45°N) in the eastern Atlantic (Figure 1) in an effort cooperative and simultaneous with the North Atlantic Study of TTO. Twenty-eight hydrographic stations were occupied to obtain, similar to TTO efforts, measurements of hydrographic and isotopic properties. The section thus extended the areal coverage provided by the TTO North Atlantic Study. However, a special task was to provide data that would allow us to study the circulation of the waters below about 3000 m depth in the northeast Atlantic. ^{14}C and ^{39}Ar data, as well as hydrographic and nutrient data, have been obtained for this purpose.

The northeast Atlantic below 3000 m basically represents a topographically enclosed deepwater basin stretched out in a north-south direction. It is separated from the West Atlantic by the Midatlantic Ridge, except for certain gaps at low latitudes—notably the Romanche Trench (0°N, 18°W), through which new water enters [*Wüst*, 1936]. Renewal from the north is believed to be small. The resulting along-basin circulation should cause decreasing radionuclide concentrations northward, owing to radioactive decay while the water flows along.

In the following, our northeast Atlantic deepwater radionuclide data set, as well as a preliminary evaluation with respect to the deep and bottom water circulation, are presented. A second aspect adressed is that, for the first time, oceanic ^{39}Ar measurements have been performed that systematically span an entire deepwater mass and can be compared to those of a more conventional radionuclide: ^{14}C. Both nuclides, as long as bomb-^{14}C can be ignored, are steady state tracers of ocean circulation. However, they differ in their ocean chemistry, in half-life (by a factor of 20), and in the degree to which the radioactive clock is reset to zero in the deepwater formation processes.

Paper number 4C1508.
0148-0227/85/004C-1508$05.00

2. HYDROGRAPHIC SITUATION

The northeast Atlantic deep and bottom water below 3000 m depth (hereinafter denoted as NEADW) exhibits the relative uniformity in hydrographic characteristics that is typical of enclosed deepwater masses. The observed, minor, along-basin gradients of temperature, salinity, and silica have been interpreted as indicative of a general northward flow regime [*Wüst*, 1936; *Metcalf*, 1969]. New water, as mentioned, enters from the West Atlantic. The dominating sill of the Romanche Trench, supposedly a major pathway of inflow, has a depth near 4000 m. The inflowing water, therefore, is derived from a depth range in the West Atlantic that is transitory between North Atlantic Deep Water (NADW) centered above it and Antarctic Bottom Water (AABW) below it [*Wüst*, 1936]. Some additional water presumably enters through the Vema fracture zone (11°N, 43°W), which has a sill depth near 4600 m, although the inflow appears to be small [*Eittreim et al.*, 1983; *Vangriesheim*, 1980]. Iceland-Scotland overflow water, which might be added from the north, appears to be restricted to depths not exceeding 3000 m [*Lee and Ellett*, 1965]. The Charlie-Gibbs fracture zone (53°N, 35°W) would be deep enough (sill depth 3600 m) to allow inflow from the West Atlantic, but observations do not support an inflow [*Harvey*, 1980]. A first-order notion of the circulation in the basin would thus be a net northward flow fed at equatorial latitudes and closed by upwelling. The purpose of the deepwater *Meteor* project is to quantify this flow and the superimposed mixing. In addition to the northward flow there is also flow from the Sierra Leone Basin southward to replenish the deep waters of the Guinea and Angola basins.

Broecker et al. [1980*a*] have shown that within the NEADW, relative to the water entering from the west, nutrients and ^{226}Ra are enriched, owing to respiration and dissolu-

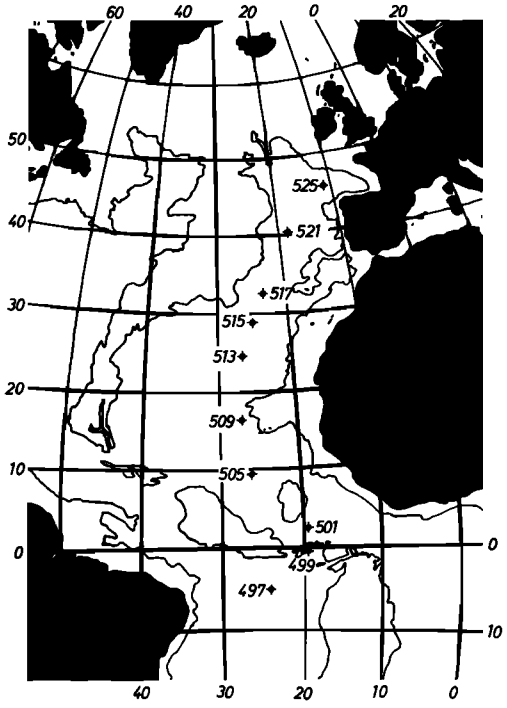

Fig. 1. Track of *Meteor*, cruise 56, leg 5, in the northeast Atlantic. Only the large-volume water-sampling stations are shown. The 4000-m isobath is indicated as an approximate boundary of the deep and bottom water.

tion effects, while oxygen and ^{14}C are depleted. These authors compared ^{14}C concentrations in the Western Basin at a typical NEADW salinity ($S = 34.88$) with NEADW values at 28°N and found an apparent aging of 80 ± 40 years. *Broecker* [1979] pointed out that NADW has considerable amounts of AABW admixed, and he presented a scheme to calculate back to the fraction actually derived from North Atlantic deepwater formation processes, which he called northern component water (NCW). His distinction, which we use below, depends on typical, and highly different, nutrient characteristics for NCW and the Southern Ocean component (SCW, southern component water), the latter being essentially young pure AABW.

3. Sample Collection

On the stations shown in Figure 1, water samples for ^{14}C and ^{39}Ar measurement were collected with Gerard-Ewing samplers (250-L volume). Contamination-free sampling was verified on the basis of consistency of the T-S relationship among these samplers as well as Niskin bottles usually tripped at in-between depths. Total inorganic carbon and dissolved gases were extracted on-board ship by using a vacuum extraction system (R. Kuntz, unpublished thesis, 1980): The seawater was acidified and sprayed into a vacuum chamber (rate 8 L/min) in which the pressure was held at water vapor pressure by removing both water and the released permanent gas through pumping. The gas was then bubbled through purified NaOH solution to trap the CO_2 for ^{14}C measurement, and the remainder was collected for ^{39}Ar and ^{85}Kr measurement. Because of amount requirements, the extracted gas from four Gerard-Ewing samplers was combined into one ^{39}Ar sample (see Table 1). These samplers usually spanned a depth interval of about 400 m. The ^{39}Ar values thus represent mean concentrations over such a depth range, while four separate ^{14}C measurements generally exist. The extraction efficiency was about 85% for CO_2 and 95% for Ar. Contamination of the extracted gas with air was examined by parallel ^{85}Kr activity measurement and was found to be small (see below).

4. ^{14}C and ^{39}Ar Measurements

4.1. ^{14}C

^{14}C concentrations were measured by gas counting on the CO_2 set free in the laboratory from the NaOH solutions [*Schoch et al.*, 1980]. A ^{14}C blank arising from the NaOH was checked and was found negligible (0.2‰ in $\Delta^{14}C$). At the desired level of precision, ^{14}C counting efficiency is affected by electronegative impurities in the counting gas that reduce the height of the signals, thus leading to a shift of the energy spectrum toward smaller energies and, therefore, to a decrease of the count rates. External gamma radiation was used to quantify the effect of impurities, the relative portion of pulses in a low-energy window being a measure of impurity content of the sample gas. The effect was calibrated in terms of ^{14}C efficiency by repeated measurements of samples of the Heidelberg sodium carbonate ^{14}C substandard [*Kromer*, 1984] that differed in impurity content. ^{14}C counter background varied as a consequence of variable cosmic ray flux but was found to be correlated with the count rate in coincidence with the cosmic ray shield counter. A background count rate normalized to the actual coincidence count rate and a counting efficiency normalized to the actual γ count rate ratio were used to calculate the $\Delta^{14}C$ value in any sample run.

The samples were usually measured in two different counters for one half-week each; this produced a statistical counting error of ±1.4‰. Accounting additionally for the estimated uncertainties of counter background and counting efficiency, we estimate the overall 1-σ error of the $\Delta^{14}C$ values to be ±2‰. This result is consistent with the apparent standard deviation (±2.1‰) of the individual ^{14}C data points from smooth ^{14}C depth profiles drawn by eye through the data points for each station. Since the samples for any station were measured in different counters and the measurements for the various stations were mixed in time, the scatter of the data in the depth profiles provides an estimate of the overall precision achieved with our procedure.

The ^{14}C data are reported in the usual $\Delta^{14}C$ notation [*Stuiver and Pollach*, 1977]. The present data refer to the 1983 recalibration of the Heidelberg sodium carbonate substandard to NBS (National Bureau of Standards) oxalid acid [*Kromer*, 1984]. The new Heidelberg calibration is 10.2‰ lower than that of previously reported ^{14}C values of this laboratory [e.g., *Roether et al.*, 1980*a*]. A comparison with the calibration of the GEOSECS (Geochemical Ocean Sections Study) ^{14}C data [*Stuiver and Östlund*, 1980] was made on the basis of the ^{14}C versus potential-temperature relationships for five pairs of nearby GEOSECS and *Meteor* stations (25 GEOSECS data points altogether, $\theta < 3$°C) in the equatorial West Atlantic and the northeast Atlantic, which gave a GEOSECS-*Meteor* difference of 1.0 ± 0.6‰ (1-σ uncertainty). In summary we believe that our data are precise to ±2‰, and that there is no detectable difference to the GEOSECS data calibration.

4.2. ^{39}Ar

The principal features of the ^{39}Ar dating method have been described previously [*Loosli*, 1983]. ^{39}Ar, a beta radioactive nuclide with a half-life of 269 years, is produced mainly by cosmic rays in the stratosphere by the ^{40}Ar (n, $2n$) process. Based on observed ^{14}C variations in tree rings, the natural variations in the atmospheric $^{39}Ar/Ar$ ratio have been esti-

TABLE 1. Measured Characteristics for ^{39}Ar Samples Along *Meteor* Track

Sample	Longitude/ Latitude, °W/°N	Depth, m	Salinity	Θ, °C	SiO_2, μm/kg	$\Delta^{14}C$, ‰	^{39}Ar, % modern	Fraction SCW, %
497/2*	24/−5	4500	34.740	0.54	110.5	−155	46 ± 4†	90
497/3	24/−5	3400	34.921	2.30	32.9	−103	56 ± 5	18
499/4	19.5/−0.5	4100	34.824	1.34	70.6	−128	53 ± 9	52
501/5	19.5/2.5	4500	34.880	1.87	50.6	−116	49 ± 4	34
505/7	26/9.5	2800	34.938	2.59	33.3	−110	53 ± 5	21
505/9	26/9.5	4600	34.889	1.91	49.7	−115	47 ± 4†	33
509/10	27/16.3	3800	34.904	2.11	47.0	−120	46 ± 7	31
515/14	25.2/28.8	4500	34.901	2.03	48.1	−120	48 ± 6	32
517/16	23.3/32.8	4500	34.907	2.07	47.0	−120	45 ± 6	31
517/17	23.3/32.8	2700	34.980	2.85	29.4	−99	57 ± 5	19
521/18	18.5/40.3	4500	34.910	2.13	46.3	−122	46 ± 5	31
521/19	18.5/40.3	2700	34.972	2.90	26.6	−91	59 ± 7	15
525/21	11.0/46.0	4300	34.909	2.14	46.3	−122	49 ± 9	30
TTO/111	17.5/37.9	5590	34.896	2.05	45.5		39 ± 4†	32

^{14}C in $\Delta^{14}C$ notation, ^{39}Ar in % modern. Silicate results courtesy of P. Brewer, Woods Hole. Values are means of values for the four Gerard samples that were combined to get one ^{39}Ar sample. The fraction of southern component water is calculated according to *Broecker* [1979], i.e., $((SiO_2)_{sample} - 10)/(125 - 10)$, respectively $((NO)_{sample} - 420)/(512\text{-}420)$, where $NO = 9NO_3 + O_2$.

**Meteor* 56 station number/^{39}Ar sample number; TTO/111, see Figure 3.

†Average of two consistent measurements.

mated to be less than 7% in the past 1000 years. A possible anthropogenic contribution by nuclear tests or nuclear industry to the present atmospheric activity is less than 5% modern. These variations are judged to be practically negligible for the usual dating purposes.

Since the specific ^{39}Ar activity is very low (100% modern = 0.107 ± 0.004 dpm/L (STP) of pure argon), it can be measured in natural argon samples by special low-level counting technique only. By operating a counting system with on-line computer control in an underground laboratory and by using high-pressure proportional counters made from specially selected copper, extremely low and stable background values have been achieved. To separate and purify the argon and krypton fractions for use as counting gas, a special gas-chromatographic procedure has been developed (U. Weidmann, unpublished thesis, 1982). High overall extraction yields have been achieved (about 90% for argon, 50–80% for krypton), so that the available gas samples yielded about 300 mL (STP) of argon which, during a counting period of about 6 weeks, produced acceptable statistical counting errors. During counting, the multichannel computer system permitted control of stability and reproducibility of the counting conditions. External calibration with gamma sources, spectrum identification, and statistical tests helped to reduce uncertainties in the ^{39}Ar results. Modern atmospheric argon was used for ^{39}Ar standardization [*Loosli*, 1983].

As the count rates for modern samples and the background are of the same magnitude, uncertainties in the value of the background could influence the results considerably. Measured pressure and time dependence of the background, but also of net standard values, were taken into account. The quoted errors include a 1-σ statistical counting error and an overall estimate of the uncertainties in the background and standard values. Relative errors of 10–14%, which correspond to about 40–55 years in ^{39}Ar age, have been obtained. Contamination of the extracted argon by air argon, checked by the ^{85}Kr content (assuming the true ^{85}Kr concentration to be negligible), was found to be between 1% and 3% and was corrected for in the ^{39}Ar results. The ^{14}C-^{39}Ar correlation of our data (see Figure 6 below) gives strong indication that the quoted ^{39}Ar errors are not underestimated.

5. ^{14}C AND ^{39}Ar SECTIONS

Figures 2 and 3 give the ^{14}C and ^{39}Ar distributions along the *Meteor* section. The ^{14}C concentrations (Figure 2) within the NEADW, i.e., from station 501 northward, below about 3500 m show but little variation. The bottom water concentrations decrease from −117‰ south of the Sierra Leone Rise (station 501) to −123‰ in the Iberian Basin (station 521)—i.e., by 6‰ only. A quite weak, but nevertheless well-documented, relative ^{14}C minimum (−123‰) appears near 4000 m depth between 15° and 40°N. Larger ^{14}C gradients exist across the Romanche Trench: Below sill depth (~4000 m), a sharp north-to-south concentration decrease (from station 501 to 497) is manifest; this is caused by the almost undiluted AABW to be found toward the bottom at station 497; while above sill depth, the north-south change is more gradual and of opposite sign (between stations 499 and 509). Upward of 3500 m and north of about 10°N, the ^{14}C concentrations rise markedly. It is believed that the contouring in Figure 2 within the NEADW is significant to ±2‰ as a result of data precision and consistency as well as of the considerable number of available data points.

For the water at or below 3000 m depth along the section a bomb-^{14}C contribution should not exceed 1‰ in $\Delta^{14}C$ because of nondetectable tritium in these waters ($\leq$0.05 TR) and a bomb-^{14}C to tritium ratio of 20‰/TR. The tritium limit (1-σ) is based on parallel tritium measurements for part of the ^{14}C samples of station 525 and from near 3000 m depth at stations farther south, as well as from repeated observations on previous cruises [*Weiss et al.*, 1976; *Roether and Weiss*, 1978; Heidelberg Tritium Laboratory, unpublished data, 1984] that consistently indicate nondetectable tritium. The 20‰/TR correspond to the 13.5‰/TR reported by *Roether et al.* [1980*b*] for deep water from North Atlantic sources in 1972, corrected for tritium decay to 1981 [see also *Broecker*, 1979].

The ^{39}Ar section (Figure 3) is consistent with the ^{14}C distri-

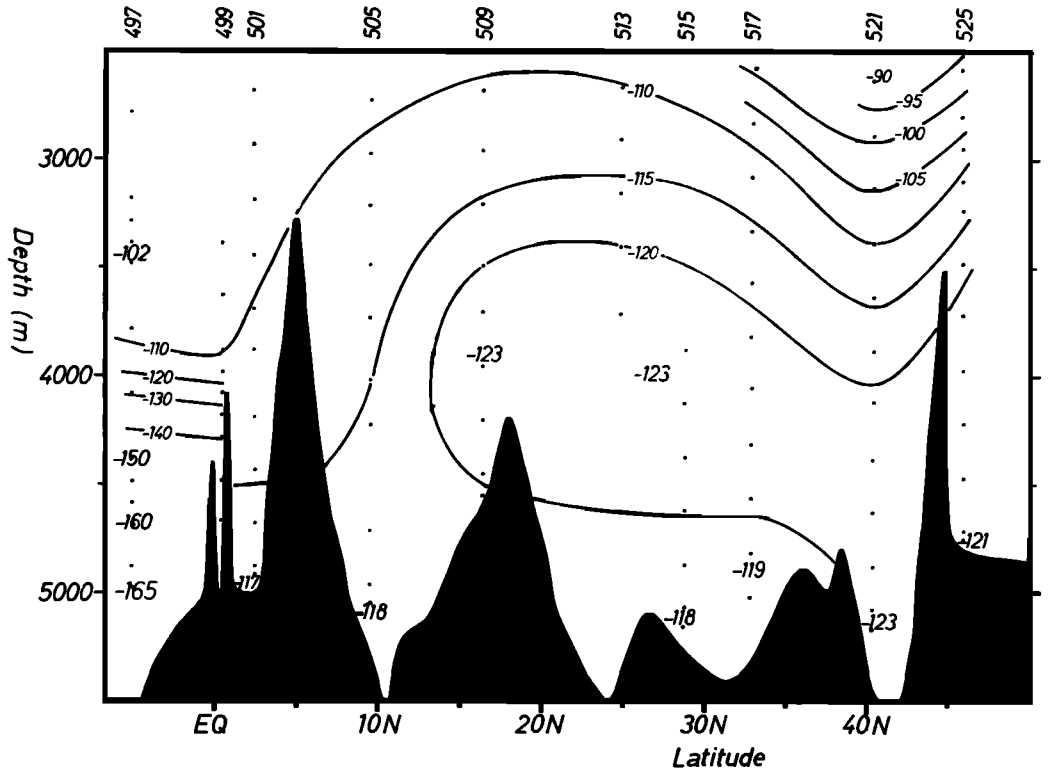

Fig. 2. The ^{14}C distribution along the *Meteor* track below 2500 m depth. Values in $\Delta^{14}C$ notation (see text), which basically is a Permille deviation from a standard. Dots indicate the position of the actual data points. The individual ^{14}C data will be published in *Radiocarbon* (B. Kromer et al., unpublished manuscript, 1985). Bottom topography is along the track and often does not correspond to deepest north-south connection.

bution. The deep samples yield ^{39}Ar values in the range of 45–49% modern; however, a horizontal gradient cannot positively be identified as a result of the less favorable resolution of the ^{39}Ar values compared to Figure 2. A low value ($39 \pm 4\%$), but still within 2 σ of the other NEADW ^{39}Ar results, was measured for sample TTO 111, collected in about 5600 m depth. Like the ^{14}C, the ^{39}Ar values from about 2800 m are higher than the deeper ones. In the vicinity of the inflow, both nuclides again yield consistent values: sample 2, consisting mainly of AABW, is lower in ^{39}Ar than sample 3, which is mainly NADW; while samples 4 and 5, as expected, show intermediate values. The general ^{39}Ar-^{14}C correlation is discussed below.

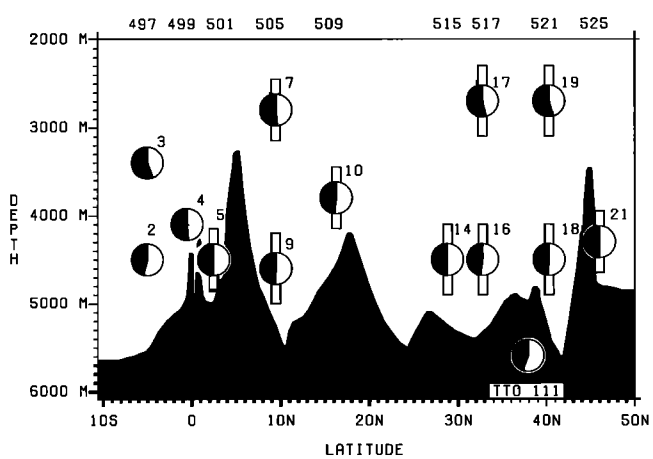

Fig. 3. The ^{39}Ar distribution. Filled fraction of circles corresponds to percent modern of ^{39}Ar concentration; for ^{39}Ar values see Table 1. The vertical bars show the depth interval from which water samples were combined to get one ^{39}Ar sample; for samples 2–4, depth interval corresponds to circle diameter. Data point without number is for sample TTO 111, collected east of the *Meteor* track during the TTO North Atlantic Study (38°N, 17,5°W, 5600 m depth).

6. Turnover of Northeast Atlantic Deep Water

The observed ^{14}C decrease northward along the section within the deeper strata of the NEADW (Figure 2), which reflects the transit time of the waters during their presumed northward flow (see section 2), is converted into an estimated turnover time as follows: We consider the waters below 4250 m, a depth that approximately coincides with that of the ^{14}C minimum, and we regard these waters as well mixed vertically. Furthermore, we take the along-basin velocity $v(x)$ in this layer of water as decreasing linearly with distance x from the upstream end, and we neglect vertical as well as horizontal mixing. The linear velocity decrease would, for example, correspond to a layer of constant cross section that loses water by uniform upwelling at the upper boundary. Because the boundary essentially coincides with the ^{14}C-minimum depth, vertical mixing should not inordinately affect the ^{14}C balance of the layer. An effect of particulate ^{14}C flux is neglected. In this highly idealized model the transit time–distance relationship for the layer is

$$t/t_0 = -\ln(1 - x/L) \qquad (1)$$

where, t_0 is turnover time ($= L/v(0)$), and L is length of basin. Figure 4 compares vertical ^{14}C averages for the layer with this relationship, and one finds that the model fits the data adequately for a turnover time of $t_0 = 33$ years. It should be noted that the stations from which the ^{14}C values in Figure 4 originate are essentially located in different basins of the

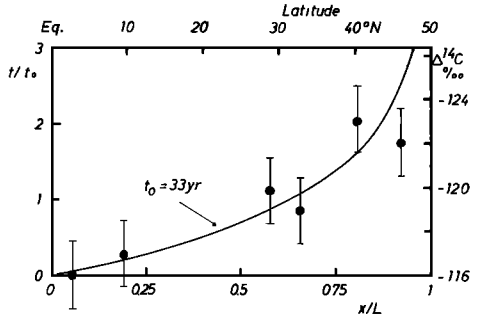

Fig. 4. Transit time versus along-basin distance relationship for a water layer with constant cross section and uniform upwelling without mixing (curve, lower and left scale) compared to the apparent ^{14}C aging observed in the waters below 4250 m depth along the *Meteor* section (upper and right scale). For explanation, see text. The ^{14}C bars, ± 1.5‰, are estimated from Figure 2.

northeast Atlantic (i.e., Sierra Leone Basin, Canary-Cape Verde Basin, etc.), so that the ^{14}C values should be largely unaffected by circulation confined within any one of these basins. The turnover time of 33 years can be converted into a water flow at the upstream end by taking into account the volume of the layer, i.e., the NEADW volume below 4250 m. Based on data reported by *Levitus* [1982], the volume is approximately $V = 5 \cdot 10^{15}$ m^3, and the flow, accordingly, is $V/t_0 \approx 4.8 \cdot 10^6$ m^3/s.

This flow should be a mixture of western Atlantic water overflowing the Romanche Trench sill and of water farther on entrained by the overflow along its downflow path into the basin (for a Vema fracture zone influence, see below). The mixing situation can be assessed from Figure 5, which gives the combined silica and ^{14}C versus potential temperature plots below 3500 m depth from stations to both sides of the Romanche Trench and in which Sierra Leone Basin bottom water, as found at station 501 of a potential temperature slightly below 1.8°C, is represented by points A and A'. The plots for the Sierra Leone Basin data are linear within the data uncertainties, and so are the ones for the western basin

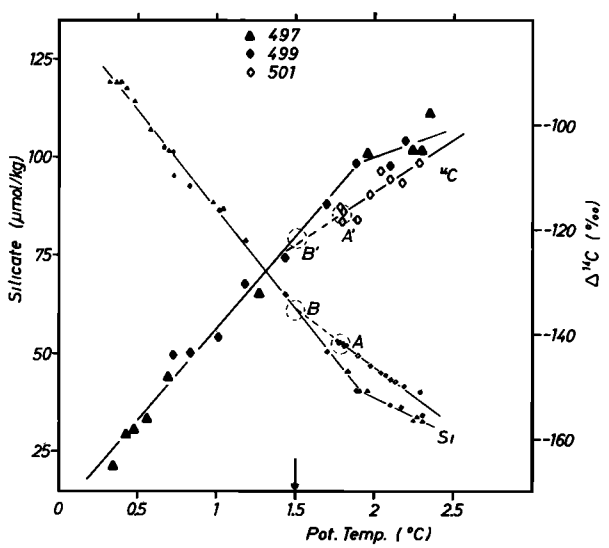

Fig. 5. Combined SiO_2 and ^{14}C versus potential-temperature plots for stations 497 and 499, representing western basin water, and station 501, representing the eastern basin (see Figure 1 for station positions). For explanation, see text. Arrow at abscissa marks the deduced potential temperature of the inflow across the Romanche Trench sill.

TABLE 2. Average Characteristics of the Deep Water That Enters the East Atlantic Across the Romanche Trench Sill

Parameter	Value
θ, °C	1.50 ± 0.05*
Salinity	34.843 ± 0.006
SiO_2, µmol/kg	62 ± 3
NO_3, µmol/kg	22.3 ± 0.6
PO_4, µmol/kg	1.58 ± 0.05
O_2, µmol/kg	249 ± 3
NO†, µmol/kg	458 ± 3
ΣCO_2, µmol/kg	2210 ± 2
$\Delta^{14}C$, ‰	−122 ± 3
Fraction SCW‡	0.44 ± 0.02

See text for explanation of table.

*Quoted uncertainties are those arising from the fit of the lines of Figure 5 or from temperature uncertainty and property-temperature correlation.

†$NO = 9NO_3 + O_2$ [*Broecker*, 1979].

‡See Table 1.

stations (stations 497 and 499) below 1.9°C. It follows that points B and B', defined by the intersection of the (extrapolated) Sierra Leone Basin and the western basin property-property lines, should represent the characteristics of the water entering from the west, provided that these properties are sufficiently conservative, which is suggested by the fast turnover of the deep water as deduced here. Data for further properties from the stations included in Figure 5 are consistent with the inferred mixing situation. The average temperature of the overflow component was determined by a statistical evaluation of the data of Figure 5, and corresponding values for other properties were obtained from the property-temperature correlations. These data, summarized in Table 2, have further been used to break up the inflowing water into northern and southern component water according to *Broecker*'s [1979] definition (see section 2), and an NCW to SCW ratio of approximately 5:4 is obtained; the SCW fraction is included in the table.

Furthermore, it is possible to tentatively convert the NEADW flow rate deduced above ($4.8 \cdot 10^6$ m^3/s) into a rate of Romanche Trench overflow by accounting for the volume increase by entrainment in the overflow process as well as for the additional southward deep flow from the Sierra Leone Basin into the Guinea and Angola basins. These basins, according to the ^{14}C data reported by *Stuiver and Östlund* [1980], have a water turnover that is similarly as fast as that for the northern basins, and therefore their effect can be approximated by simply increasing the flow after entrainment proportional to their additional volume ($\sim 2.5 \cdot 10^{15}$ m^3 below 4250 m), i.e., to $7.2 \cdot 10^6$ m^3/s. Entrainment can be expected to largely occur early on in the overflow process (see discussion by *Stalcup et al.* [1975] and *Ribbat et al.* [1976] for the deep Caribbean inflow), and the entrained component should thus have an average temperature corresponding to a depth not far below sill depth. Taking the effective depth as 4100 m, the potential temperature (average of station 501 and GEOSECS station 111 at 2°N, 14°W [*Bainbridge*, 1981]) of the entrained component becomes 2.0°C. The average temperature for the same stations below 4900 m, which might represent that of the fresh overflow after entrainment, is approximately 1.75°C. These temperatures, together with that for the original overflow (1.5°C, see Table 2), point to a 1:1 ratio of original overflow to entrained component, which in turn leads to an estimated overflow rate of $3.6 \cdot 10^6$ m^3/s.

Such flow is much larger than the inflow of $(0.25 \pm 0.2) \cdot 10^6$

TABLE 3. Flow Rate Estimates

Parameter	Value
Source flow into NEADW	$4.8 \cdot 10^6$ m^3/s*
Ratio overflow to entrained component	1 : 1†
Romanche Trench overflow	$3.6 \cdot 10^6$ m^3/s‡

For explanation of table, see text.

*Volume ($5 \cdot 10^{15}$ m^3) divided by turnover time (33 years (Figure 4)).

†Based on component potential temperatures: entrained component, 2.0°C; young Sierra Leone bottom water, 1.75°C; overflow, 1.5°C (Table 2).

‡NEADW source flow increased 1.5 times to account for additional deep southward flow and corrected for entrainment, i.e., $0.5 \cdot 4.8 \cdot 10^6$ m^3/s $\cdot$ $(5 \cdot 10^{15}$ m^3 + $2.5 \cdot 10^{15}$ m$^3)/(5 \cdot 10^{15}$ m^3).

m^3/s through the Vema fracture zone according to *Vangriesheim* [1980], so that our ignoring any flow above appears justified. A rough upper limit for an inflow from the north is obtained by assuming that, despite the general northward ^{14}C decrease (Figure 2), all ^{14}C decay within the West European and Iberian basins in the depth range below 4250 m, as considered above, is compensated for by inflow from the north. Because any such inflow has considerably higher ^{14}C concentration (−67‰, see Table 4), the required flow is $0.06 \cdot 10^6$ m^3/s only.

Our flow rate estimates are summarized in Table 3. It is obvious that these rates are preliminary and that a more refined evaluation of our data is called for. Qualitatively, however, there can be no doubt that the NEADW turnover is quite fast and the Romanche Trench overflow large and that this overflow predominates over any inflow through the Vema fracture zone or from the north. It can be presumed that the return flow occurs through upwelling and is extended over a considerable portion of the East Atlantic. We believe that the resulting redistribution of water might have a noticeable effect on the hydrographic structure of the West Atlantic deep water below about 3000 m depth.

7. ^{39}Ar-^{14}C Correlation

This section considers the ^{39}Ar-^{14}C data consistency and potential uses of oceanic ^{39}Ar data. Internal consistency of the ^{14}C and ^{39}Ar results is demonstrated by Figure 6, which gives

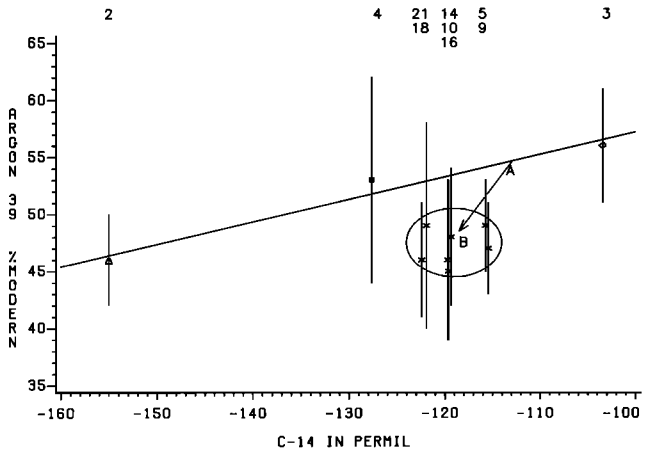

Fig. 6. ^{39}Ar versus ^{14}C plot for the deep *Meteor* samples. ^{39}Ar sample numbers are given at top, ^{39}Ar error bars are shown. ^{14}C is average of the four samples combined for ^{39}Ar measurement (see Table 1). Line is linear fit for samples 2, 3, and 4. Arrow A to B indicates radioactive decay. For explanation, see text.

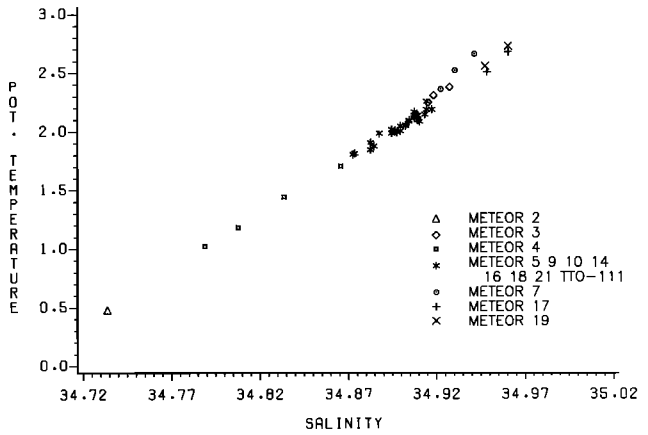

Fig. 7. Potential temperature-salinity diagram for those Gerard samples used for the ^{39}Ar measurements of Figure 6. For ^{39}Ar sample numbers, see Table 1 and Figure 3.

the ^{39}Ar-^{14}C correlation of our data. An apparent mixing line, disregarding the considerable error margins, is drawn through data points 2, 3, and 4, which represent a vertical profile just upstream from the Romanche Trench inflow (see Figure 3). The points are those in the range denoted B and are from the enclosed deep basin, and they all fall below the mixing line in accordance with the expected radioactive decay. Figure 7 characterizes the same data points by their T-S diagram, samples that were combined for ^{39}Ar measurement being represented individually. Apparently, data points 2–4 of Figure 6 belong to a linear T-S regime, so that the notion of a mixing line in Figure 6 is appropriate. In Figure 7 the samples from the enclosed deep basin, shown as asterisks, fall into a comparably restricted T-S range.

Our data upstream from the Romanche Trench inflow can be used to extrapolate to the equatorial ^{14}C and ^{39}Ar concentrations of the two mentioned source water components (NCW and SCW, see section 2). Figure 8 indicates the ^{14}C extrapolation by means of a ^{14}C versus fraction-SCW plot. The plot is sufficiently linear to allow a meaningful extrapolation to the pure components, which are found to have ^{14}C

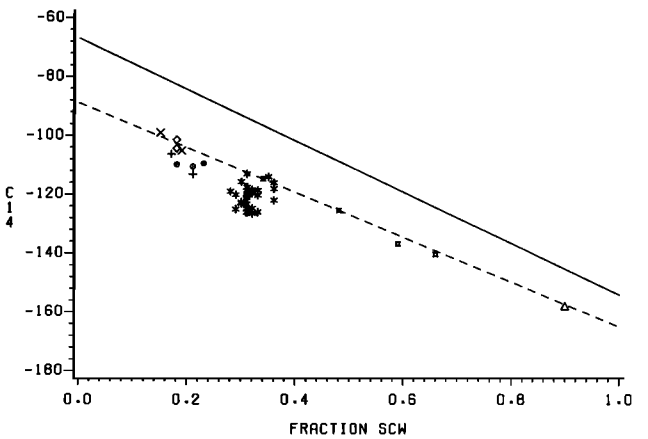

Fig. 8. ^{14}C versus fraction southern component water for the samples of Figure 6; signs as in Figure 7. Fraction SCW was calculated according to the scheme of *Broecker* [1979], applying NO and silicate (see Table 1). The dashed line shows the linear fit for the samples collected near the Romanche Trench (numbers 2, 3, and 4). The values in the basin are below the line as a result of aging. The solid line represents, for comparison, mixing without aging between source NCW and SCW (Table 4).

TABLE 4. Summary of Measured and Estimated ^{39}Ar and ^{14}C Concentrations for Pure SCW (equal to Undiluted AABW) and Pure NCW at the Equator and in the Source Areas

	$\Delta^{14}C$, ‰		^{39}Ar, % modern	
	Equator	Source	Equator	Source
SCW	-165 ± 2*	-154†	45 ± 5*	60 ± 7‡
NCW	-89 ± 2*	-67†	59 ± 6*	85 ± 5¶

*Extrapolated from observations (see Figures 6 and 8 and text); quoted errors are linear regression uncertainties, taking into account the measurement errors.

†*Broecker and Peng* [1982].

‡Decay corrected from equatorial value (see text).

¶*Smethie et al.* [1983].

concentrations of −89‰ and −165‰. The corresponding ^{39}Ar values are obtained from the equatorial ^{39}Ar-^{14}C correlation line of Figure 6. These ^{39}Ar and ^{14}C concentrations are entered into Table 4 together with literature values for young NCW and SCW. For the NCW the apparent aging from the formation area to the equator is consistent for the two nuclides (190 ± 30 years for ^{14}C and 140 ± 40 years for ^{39}Ar). It is concluded from these findings that the ^{39}Ar distribution of the deep waters of the North Atlantic, within the analytical ^{39}Ar errors, is fully consistent with the ^{14}C distribution. No ^{39}Ar data are available for SCW or young AABW, but a decay correction on the basis of the apparent ^{14}C aging (105 ± 40 years) applied to the above-derived SCW ^{39}Ar concentration at the equator ($45 \pm 5\%$ modern) yields $60 \pm 7\%$ modern (see Table 4). This value should be a valid estimate for young AABW.

The ^{14}C and ^{39}Ar values for SCW and NCW of Table 4 are entered into another extended ^{39}Ar versus ^{14}C plot in Figure 9 together with the apparent mixing line of Figure 6 and the related observational data. Also shown are aging lines (dotted) for the SCW and NCW as well as a hypothetical one for the aging of water from the prenuclear oceanic surface water pool ($\Delta^{14}C = -40$‰ [*Broecker*, 1979], $^{39}Ar = 100\%$ modern) without any further mixing. It is apparent that all observed points are distinctly above the latter line. There are two effects that contribute to the observed deviation from this line,

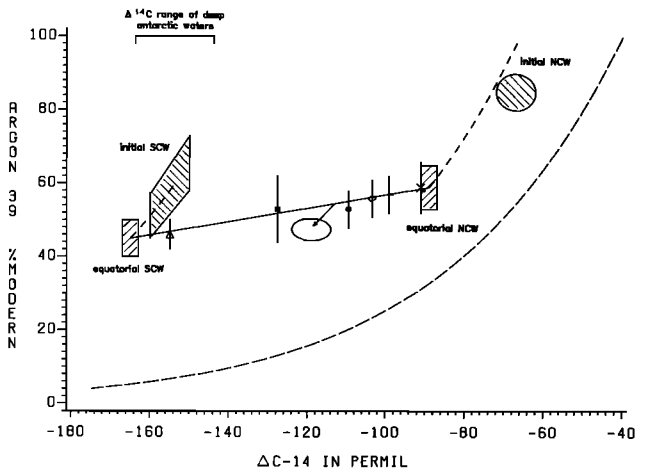

Fig. 9. Extended ^{39}Ar versus ^{14}C plot. Hatched areas represent the data of Table 4. Dashed lines represent lines of parallel ^{14}C and ^{39}Ar decay without mixing. For explanation, see text. The $\Delta^{14}C$ range of deep Antarctic waters [*Weiss et al.*, 1979] is shown for comparison.

namely, mixing of waters of different age in view of the curvature of any simultaneous ^{39}Ar-^{14}C aging line and more efficient raising of ^{39}Ar in the actual formation of deep water.

The second effect arises because the characteristic time of isotopic equilibration with the atmosphere of a pool of water in contact with the air-water interface is on the order of 100 times faster for ^{39}Ar than for ^{14}C [*Broecker and Peng*, 1974]. It appears from their discussion that in the convective oceanic surface layer ^{39}Ar concentrations should generally approach 100% modern. The first effect is, of course, small as long as the age range is small, such as between initial and equatorial SCW in Figure 9. Therefore by measuring both ^{39}Ar and ^{14}C in all relevant components that combine to form a certain deep water mass, as well as in the product of this process, the effect of more efficient raising of ^{39}Ar should become resolvable.

The situation may be illustrated for the case of the formation of AABW in the Weddell Sea. The AABW is supposed to be largely derived from the so-called warm deep water (WCW) with a core depth in the Weddell Sea of about 500 m [*Weiss et al.*, 1979]. According to these authors, a large fraction (0.62) of the WDW enters the AABW directly, while the remainder (0.38) becomes subjected to surface layer processes before sinking down. Despite this surface layer involvement, however, the WDW ^{14}C concentration of −158‰ reported by *Weiss et al.* [1979] is virtually indistinguishable from the −154‰ for young AABW (Table 4). On the other hand the water conversion processes in the Weddell Sea appear to be such [*Gill*, 1973] that the surface-transformed fraction of the water should have sufficient contact with the atmosphere to approach 100% modern in ^{39}Ar and that in the subsequent mixing of this fraction with original WDW, by which the bottom water is actually formed, there is no contact with the atmosphere so that no additional ^{39}Ar should be added. In a first approximation, therefore, one estimates that WDW should have an ^{39}Ar concentration around 35% modern ($35\% = (60\% - 0.38 \cdot 100\%)/0.62$). Consequently, in this approximation, considering also the error margins (±7% modern) for the 60% modern value of young AABW, the conversion of WDW to AABW is expected to be accompanied by an ^{39}Ar increase of 20–30% modern. Such increase, which certainly can be regarded as a rough estimate only, is in fact substantial, relative to the mentioned related ^{14}C increase, and moreover can be well resolved by ^{39}Ar data.

A special aspect is that, because the slowly equilibrating ^{14}C and the faster ^{39}Ar bracket the air-sea equilibration for CO_2, a detailed ^{14}C-^{39}Ar comparison along the lines sketched here can be a tool to quantify the fossil fuel uptake in the deepwater source regions [see also *Broecker et al.*, 1980*b*].

8. Conclusions

The foregoing ^{14}C data resolve the large-scale structure in the northeast Atlantic deep and bottom water below 3000 m (NEADW) to ±2‰, and they place the convective renewal of the deepest strata of these waters in the vicinity of 30 years. Together with hydrographic and nutrient data, they allow us to define the stratum from which, as well as a preliminary rate at which, new water from the western Atlantic enters through the Romanche Trench. A more quantitative evaluation of circulation and mixing in the NEADW, considering also a possible long-term nonstationarity of the circulation, is in progress (R. Schlitzer, unpublished thesis, 1984).

From our data and literature values we derive the aging of the Atlantic deep waters below 2500 m from their northern

and southern formation areas to the equator, and estimate the ^{39}Ar concentration of young Antarctic Bottom Water. Not suprisingly, the age resolution of the ^{39}Ar results is less than that for ^{14}C. However, the observed ^{39}Ar distribution is fully consistent with that of ^{14}C. This is an important finding, as it provides a sound basis for future oceanic ^{39}Ar work.

The general ^{39}Ar-^{14}C relationship in the ocean appears to be affected by nonlinear effects of mixing of waters of a different aging history and by more efficient raising of ^{39}Ar relative to that of ^{14}C in the deepwater formation processes. The efficient raising of ^{39}Ar for the case of AABW formation in the Weddell Sea is estimated from our data. It is envisaged that these effects might be a focus in future oceanic ^{39}Ar work.

Acknowledgments. The field work of cruise F/S *Meteor* number 56 was funded by the Deutsche Forschungsgemeinschaft. We are grateful to W. Feldmann, master, and the crew of the F/S *Meteor* for their cooperation and friendly assistance in the sampling efforts at sea. We furthermore appreciate the enthusiastic support of the scientific crew, which was an indispensable component of the success of the present project. H. Schoch-Fischer and B. Kromer were in charge of the ^{14}C measurements at the Heidelberg laboratory. The nutrient measurements were carried out by Z. Mlodzinska on behalf of P. Brewer of Woods Hole Oceanographic Institution, Woods Hole, Massachusetts. We acknowledge the help of the TTO cruise, especially of W. S. Broecker and W. M. Smethie, Jr., in providing the TTO ^{39}Ar sample included in Table 1 and Figure 3.

REFERENCES

Bainbridge, A. E., GEOSECS Atlantic Expedition, vol. 1, Hydrographic Data, 1972–1973, report, Nat. Sci. Found., Wash., D. C., 1981.

Broecker, W. S., A revised estimate for the radiocarbon age of North Atlantic Deep Water, *J. Geophys. Res., 84*, 3218–3226, 1979.

Broecker, W. S., and T. H. Peng, Gas exchange rates between air and sea, *Tellus, 26*, 21–35, 1974.

Broecker, W. S., and T.-H. Peng, *Tracers in the Sea*, 690 pp., Lamont-Doherty Geophysical Observatory, Palisades, N. Y., 1982.

Broecker, W. S., T. Takahashi, and M. Stuiver, Hydrography of the central Atlantic, 2, Waters beneath the two-degree discountinuity, *Deep Sea Res., 27*, 397–419, 1980*a*.

Broecker, W. S., T.-H. Peng, and T. Takahashi, A strategy for the use of bomb produced radiocarbon as a tracer for the transport of fossil fuel CO_2 into the deep-sea source regions, *Earth Planet. Sci. Lett., 49*, 463–468, 1980*b*.

Eittreim, S. L., P. E. Biscaye, and S. S. Jacobs, Bottom water observations in the Vema fracture zone, *J. Geophys. Res., 88*, 2609–2614, 1983.

Gill, A. E., Circulation and bottom water production in the Weddell Sea, *Deep Sea Res., 20*, 111–140, 1973.

Harvey, J. G., Deep and bottom water in the Charlie Gibbs fracture zone, *J. Mar. Res., 38*, 173–182, 1980.

Kromer, B., Recalibration of Heidelberg ^{14}C laboratory data, *Radiocarbon, 26*, 148, 1984.

Lee, A., and D. Ellett, On the contribution of overflow water from the Norwegian Sea to the hydrographic structure of the North Atlantic Ocean, *Deep Sea Res., 12*, 129–142, 1965.

Levitus, S., Climatological Atlas of the World Ocean, *Prof. Pap. 13*, Nat. Oceanic Atmos. Admin., Rockville, Md., 1982.

Loosli, H. H., A dating method with ^{39}Ar, *Earth Planet. Sci. Lett., 63*, 51–62, 1983.

Metcalf, W. G., Dissolved silicate in the deep North Atlantic, *Deep Sea Res., 16*(suppl.), 139–145, 1969.

Ribbat, B., W. Roether, and K. O. Münnich, Turnover of Eastern Caribbean deep water from C-14 measurements, *Earth Planet. Sci. Lett., 32*, 331–341, 1976.

Roether, W., and W. Weiss, A transatlantic tritium section near 40°N, *"Meteor" Forschungsergeb., Reihe A, 20*, 101–108, 1978.

Roether, W., K. O. Münnich, B. Ribbat, and J. L. Sarmiento, A transatlantic ^{14}C-section near 40°N, *"Meteor" Forschungsergeb., Reihe A, 21*, 57–69, 1980*a*.

Roether, W., K. O. Münnich, and H. Schoch, On the ^{14}C to tritium relationship in the North Atlantic Ocean, *Radiocarbon, 22*(3), 636–646, 1980*b*.

Schoch, H., M. Bruns, K. O. Münnich, M. Münnich, A multi counter system for high precision carbon-14 measurements, *Radiocarbon, 22*(2), 442–447, 1980.

Smethie, W. M., H. H. Loosli, and U. Weidmann, Argon 39 and krypton 85: New tracers of water mass formation in the Greenland and Norwegian seas, paper presented at meeting of Int. Union Geod. Geophys., Hamburg, August 15–27, 1983.

Stalcup, M. C., W. G. Metcalf, R. G. Johnson, Deep Caribbean inflow through the Anegada-Jungfern Passage, *J. Mar. Res., 33*(suppl.), 117, 1975.

Stuiver, M., and H. A. Pollach, Discussion: Reporting of ^{14}C data, *Radiocarbon, 19*, 253–258, 1977.

Stuiver, M., and H. G. Östlund, GEOSECS Atlantic radiocarbon, *Radiocarbon, 22*, 1–24, 1980.

Vangriesheim, A., Antarctic bottom water flow through the Vema fracture zone, *Oceanol. Acta, 3*(2), 199–207, 1980.

Weiss, W., W. Roether, and G. Bader, Determination of blanks in low-level tritium measurement, *Int. J. Appl. Radiat. Isotop., 27*, 217–225, 1976.

Weiss, R. F., H. G. Oestlund, and H. Craig, Geochemical studies in the Weddell Sea, *Deep Sea Res., 26*, 1093–1120, 1979.

Wüst, G., Das Bodenwasser und die Gliederung der Atlantischen Tiefsee, *Wiss. Ergeb. Dtsch. Atl. Exped. "Meteor" 1925–1927, 6*(1), 3–106, 1936.

P. Kalt, H. H. Loosli, and U. Weidmann, Physikalisches Institut, Universität Bern, Sidlerstrasse 5, CH-3012 Bern, Switzerland.

W. Roether and R. Schlitzer, Institut für Umweltphysik, Universität Heidelberg, Im Neuenheimer Feld 366, D-69 Heidelberg, Federal Republic of Germany.

(Received February 13, 1984;
revised November 11, 1984
accepted December 11, 1984.)